Published in final edited form as:
Brain Res. 2012 June 15; 1460C: 12–24. doi:10.1016/j.brainres.2012.04.002.

Impaired motor coordination and disrupted cerebellar architecture in Fgfr1 and Fgfr2 double knockout mice

Karen Müller Smith[a,*], **Theresa L. Williamson**[b,*], **Michael L. Schwartz**[c], and **Flora M. Vaccarino**[a,b]

Karen Müller Smith: Karen.smith@yale.edu; Theresa L. Williamson: theresa.williamson@yale.edu; Michael L. Schwartz: Michael.schwartz@yale.edu; Flora M. Vaccarino: flora.vaccarino@yale.edu

[a]Child Study Center, Yale University, 230 South Frontage Rd, New Haven, CT 06520,USA

[b]Child Study Center, Yale University, 230 South Frontage Rd, New Haven, CT 06520,USA

[c]Department of Neurobiology, Yale University, 333 Cedar St, New Haven, CT 06520,USA

[d]Child Study Center, and Department of Neurobiology, Yale University, 230 South Frontage Rd, New Haven, CT 06520, USA

Abstract

Fibroblast growth factor receptor (FGFR) signaling determines the size of the cerebral cortex by regulating the amplification of radial glial stem cells, and participates in the formation of midline glial structures. We show that Fgfr1 and Fgfr2 double knockouts (FGFR DKO) generated by Cre mediated recombination driven by the human *GFAP* promoter (*hGFAP*) have reduced cerebellar size due to reduced proliferation of radial glia and other glial precursors in late embryonic and neonatal FGFR DKO mice. The proliferation of granule cell progenitors (GCPs) in the EGL was also reduced, leading to reduced granule cell numbers. Furthermore, both inward migration of granule cells into the inner granule cell layer (IGL) and outward migration of GABA interneurons into the molecular layer (ML) were arrested, disrupting layer and lobular morphology. Purkinje neurons and their dendrites, which were not targeted by Cre mediated recombination of Fgf receptors, were also misplaced in FGFR DKO mice, possibly as a consequence of altered Bergmann glia orientation or reduced granule cell number. Our findings indicate a dual role for FGFR signaling in cerebellar morphogenesis. The first role is to amplify the number of granule neuron precursors in the external granular layer and glial precursor cells throughout the cerebellum. The second is to establish the correct Bergmann glia morphology, which is crucial for granule cell migration. The disrupted cerebellar size and laminar architecture resulting from loss of FGFR signaling impairs motor learning and coordination in FGFR DKO mice.

Keywords

Fibroblast Growth Factor; Cerebellum; granule neurons; proliferation; migration; Bergmann glia

Correspondence to: Flora M. Vaccarino, flora.vaccarino@yale.edu.

*These authors contributed equally to this work

5. Authors' contributions

KMS and TLW designed and performed research, analyzed data and contributed to writing the manuscript; MLS analyzed data; FMV designed research, contributed to writing the manuscript and supervised the project. All authors have approved the final article.

1. Introduction

A number of Fibroblast Growth Factor (FGF) receptor ligands are expressed in the cerebellum during development. FGF8, FGF17, and FGF18 are expressed at the isthmus, just rostrally to rhombomere 1, from which the cerebellum will later arise. The *Fgf8* gene is crucial in establishing and maintaining the isthmus as a patterning center (Joyner et al., 2000; Sato and Nakamura, 2004; Zervas et al., 2004) and for maintaining sustained Ras/MAPK signaling and *Gbx2* gene expression which are crucial for cerebellar development (Li et al., 2002; Liu et al., 1999; Liu et al., 2003; Martinez et al., 1999; Sato and Nakamura, 2004). Indeed, the disruption of *Fgfr1* gene functioning in mouse at neural plate stage of development results in deletion of the inferior colliculi in the posterior midbrain and the vermis of the cerebellum (Trokovic et al., 2003).

While the fate of rhombomere 1 as distinct from the mesencephalon is established early, the formation and patterning of the cerebellum occurs over a more extended time period. The cerebellum is composed of several cell types occupying distinct layers: the cerebellar nuclei (CN) in the white matter, whose cells receive Purkinje cell fibers and project to outside regions; the internal granular layer (IGL) harboring the granule cells and several types of interneurons; the Purkinje cell layer (PL), the location of the Purkinje neurons and Bergmann glia cell bodies; and the molecular layer (ML), which is relatively cell-free and contains the axons and dendrites of granule and Purkinje neurons, respectively, and local circuit GABAergic interneurons. In mouse, Purkinje neurons are first born at embryonic day 11 (E11) from radial glial cells of the IV ventricle. Granule cells arise from cells of the rhombic lip, which also appear to have radial glial character (Schuller et al., 2008; Spassky et al., 2008). During embryonic development, granule cell precursors (GCPs) migrate from the rhombic lip across the surface of the neural tube to form the external molecular layer (EGL) on the cerebellar surface, where they acquire neuronal fate and subsequently become postmitotic. Postnatally, granule cells migrate inward from the EGL, through the ML, to form the IGL. This process begins after birth and is completed around P10–P12. The interneurons of the IGL develop prenatally, whereas ML interneurons mostly develop postnatally, from astroglial stem cells located in the cerebellar white matter (Maricich and Herrup, 1999; Milosevic and Goldman, 2004; Silbereis et al., 2009).

Previous work on FGFs in the cerebellum has shown that FGFR1 and FGFR2 are expressed throughout cerebellar folia, especially in the PL, at the interface between the IGL and the ML (Lin et al., 2009). The FGF ligands that pattern the isthmic region cease to be expressed by mid-embryogenesis and little is known about the role of FGFR signaling in the morphogenesis of the cerebellum. During the growth and patterning of the cerebellum, *engrailed* genes, Notch, bone morphogenetic protein (BMP) and Sonic hedgehog (Shh) signaling are all known to play essential roles (Cheng et al.; Lutolf et al., 2002; Machold et al., 2007; Rios et al., 2004). Specifically, *engrailed* is required for normal foliation, Notch for the timing of neuronal differentiation and proper alignment of Bergmann glia (Komine et al., 2007; Solecki et al., 2001), and Shh for the proliferation of GCPs (Wechsler-Reya and Scott, 1999). Further, FGF signaling has been suggested to be an upstream inhibitor of the Shh proliferative response (Fogarty et al., 2007). It has been shown that FGF9 is expressed in the early postnatal cerebellum and is required for the proper migration of cerebellar granule neurons, possibly through a requirement for FGF9 in the development of Bergmann glia (Lin et al., 2009). However, whether the role of FGF signaling is circumscribed to Bergmann glia and granule cell migration, or whether it involves other cell types is unclear, and the cellular mechanisms that characterize the action of FGFs in cerebellar development remain to be elucidated. Here, we show that the conditional deletion of both FGFR1 and FGFR2 results in decreased cerebellar volume and disrupted cerebellar layer morphology.

FGFR mutant animals also have abnormal motor learning. We identify two series of events by which FGFR signaling exerts a determining influence upon cerebellar morphogenesis: a regulation of the polarity of Bergmann glial cells, secondarily causing a migration defect, and a stimulation of the proliferation of precursors for both ML interneurons and GCs.

2. Results

2.1 Conditional deletion of Fgfr1 and Fgfr2 results in decreased cerebellar volume and abnormal morphology

The *hGFAP-Cre* driver has been shown to effectively disrupt *loxP*-containing alleles of *Fgfr1* and *Fgfr2 (Fgfr1*^{f} and *Fgfrz*^{f}*)* in the brain, and its effects on the development of the dorsal telencephalon are described elsewhere (Ohkubo et al., 2004; Smith et al., 2006; Stevens et al., 2010b). Recombination induced via *hGFAP-Cre* was previously reported to begin around E13.5–E14.5 in cerebellar radial glia throughout the EGL, the rhombic lip, and in the cerebellar anlage (Marino et al., 2000; Schuller et al., 2008; Zhuo et al., 2001). The cellular pattern of Cre-mediated recombination in the cerebellum was confirmed by using β-gal reporter staining in *hGFAP-Cre* mice carrying the *Rosa26R* reporter gene (Figure 1). We observed robust β-gal immunoreactivity in the rhombic lip and EGL, showing that GCPs are targeted by *hGFAP-Cre* in E16.5 embryos (Figure 1A,B). We performed three-color immunofluorescence to determine whether β-gal expression was detectable in Purkinje neurons (calbindin), cerebellar glia (Blbp), or both. β-gal immunofluorescence was present in Blbp labeled cell bodies, but not in calbindin labeled cells at E16.5 (Figure 1A–D). The data suggest that in *hGFAP-Cre;Fgfr1*$^{f/f}$*;Fgfr2*$^{f/f}$ double knockout (hereafter referred to as FGFR DKO) mice, the FGFR genes were conditionally deleted in the cerebellar anlage beginning at mid-embryogenesis in cerebellar glia, but not in Purkinje neurons. Detection of X-Gal staining in P7 animals revealed extensive recombination of the ROSA26R locus in the cerebellum of FGFR DKO animals (Figure 1E,F).

A whole mount comparison of the brains of FGFR DKO mice and *Fgfr1*$^{f/f}$*;Fgfr2*$^{f/f}$ Cre-negative control littermates revealed a drastic decrease in size of the FGFR DKO cerebellum, in both the vermis and the hemispheres (Figure 2A,B). Cresyl violet staining on sagittal sections was performed in order to examine the gross morphological organization of the cerebellar folia and their layers in adult (3 month-old) mice. Control cerebella contain distinct folia with three characteristic cerebellar layers, including the inner white matter, the cell-dense IGL, and an area poor in cell bodies, referred to as the ML (Figure 2C,E,H,and I). The folia of the FGFR DKO mutants were less well defined, and it was difficult to assign defining numbers to corresponding folia in P14 and adult mice (Figure 2D,F,K, and L). Furthermore, the cerebellar layering appeared disrupted in FGFR DKO, with poor demarcation of the ML from the IGL and dense clusters of cells evident within the ML (Figure 2D,F,K, and L). This phenotypic outcome was not observed in *Fgfr1* or *Fgfr2* single mutants (data not shown).

Cresyl violet analysis was also performed at P7, a critical time point for cerebellar development, when the granule cells are migrating from the EGL towards the IGL. At this time, the EGL appears as a cell-dense region on the external surface of the cerebellar anlage, while the internal regions show relatively lighter cresyl violet staining except for the PL (Figure 2G). At P7, the FGFR DKO cerebellum was grossly reduced in size, and the EGL and PL appeared discontinuous (Figure 2J). By P14, the control cerebellum has distinct IGL, PL and ML, whereas in the mutant cerebellum cells were scattered throughout the cerebellum, the lobules were indistinct and the ML was filled with cells (Figure 2H,K). The developmental disruption of cell distribution persisted into adulthood, and interestingly there was a gradient of abnormalities, with anterior regions relatively more disrupted and posterior regions retaining a semblance of cerebellar architecture (Figure 2E,F, **arrows**).

2.2 Granule cells are dispersed throughout the presumptive molecular and granular layers

Immunohistochemistry using the NeuN antibody confirmed that the pockets of cells found dispersed throughout the ML of the adult cerebellum in mutants were most likely granule cell neurons (Figure 3A,B). Neurons were scattered throughout the folia of mutant cerebella with virtually absent demarcation between ML and IGL, whereas in the control mice a distinct neuron-dense IGL and neuron-poor ML were formed (Figure 3A–D). In order to further confirm whether these NeuN positive cells were granule neurons, we used a calretinin antibody. In control mice, immunostaining for calretenin displayed the characteristic arrangement of calretinin-positive cell bodies in the IGL, while the ML was devoid of calretinin stained cell bodies and was rich in calretinin-positive fibers (Figure 3E,G). In comparison, the mutants did not have a defined calretinin stained IGL. Instead, there were calretinin-positive cell pockets throughout the disorganized layers of the cerebellum, including the presumptive ML (Figure 3F,H). Furthermore, concurrent immunostaining for parvalbumin (PV), known to be present in Purkinje, stellate and basket GABAergic neurons normally present in the PL and ML (Figure 3E–H, arrows) (Schwaller et al., 2002), revealed that the pockets of abnormally placed cells in the ML did not contain these cellular subtypes. Rather, PV+ stellate and basket cells were mostly displaced in the inner layer, the putative IGL. Furthermore, a distinct PL was not observed in the mutant.

2.3 Cerebellar inhibitory cells are unable to reach the molecular layer in FGFR DKO mice

In order to further examine the GABAergic interneuron populations of the cerebellum, we crossed the GAD67-GFP knock-in allele (Tamamaki et al., 2003) into the FGFR DKO strain. This allele labels all interneuron populations with GFP, allowing us to compare the interneuron populations of control and FGFR DKO mice (Figure 4A,B). In adult control animals, the small stellate and basket cell interneurons in the ML (Figure 4A, **arrowheads**), as well as the large cell bodies of the Purkinje neurons in the PL (Figure 4A, **arrows**), were labeled with GFP. Also visible in control mice were the sparse cell bodies of Golgi interneurons in the IGL, typically located close to the Purkinje layer (open arrows). In FGFR DKO mice, the small interneurons in the ML were greatly reduced in number, while the presumptive IGL contained a large number of GFP+ GABAergic cell bodies (Figure 4B, **arrows, open arrows and arrowheads**). We examined immature interneuron precursors in the developing cerebellum by staining for Pax2 and Mash1 at P7 in control and FGFR DKO mice (Figure 4C,D). As previously reported (Silbereis et al., 2009), both Pax2 positive and Mash1 positive cells were visible in the white matter of the cerebellum, while only Pax2 positive post-migratory cells were visible in the developing ML (Figure 4C). The number of Pax2 positive cells in the ML of DKO mice appeared reduced in comparison to control mice (Figure 4D).

The PL appears to be missing as an organized cell layer in adult FGFR DKO mice. Indeed, the Purkinje cells did not align to form a clear layer, but were dispersed in the presumptive IGL with cell bodies located at an increased distance to the ML, as shown by immunostaining with calbindin, a molecular marker for Purkinje cells (Figure 4E,F). This phenotype appears as early as E16, where calbindin positive cell bodies are present deeper within the cerebellar anlage in FGFR DKO mice compared to controls (Figure 1A,B). Also, the dendrites of Purkinje cells in adults mice were extremely disorganized and lacked parallel alignment when entering the molecular layer in the mutant cerebellum (Figure 4F). Purkinje cells are born on E11–E12, well before the onset of *hGFAP-Cre* mediated recombination, but migrate to the cerebellar cortex over a more extended period (E13–E17) (Yuasa et al., 1991). The absence of Cre targeting to Purkinje neuron is demonstrated in Figure 1. Thus, the Purkinje layer disorganization is likely a secondary migratory defect.

2.4 Reduced and disorganized Bergmann glia may disrupt granule cell migration

The observation of unevenly distributed cells between what should have been the primitive EGL and the IGL beginning at P14 suggested that the migratory process for GCs was disrupted when FGF signaling was decreased and led us to further evaluate the mechanisms leading to granule cell maldevelopment. During postnatal cerebellar development, granule cells located in the EGL migrate along the Bergmann glia fibers to their location in the IGL (Gasser and Hatten, 1990; Hatten, 1999). Bergmann glia have also been suggested to serve as a putative stem cell population in the cerebellum (Alcock et al., 2007) that continues to divide in the postnatal period and expresses Sox2 and BLBP (Figure 5). The number of Sox2 as well as BLBP positive glial cells was greatly reduced in the cerebellum of P7 FGFR DKO mice compared to control littermates, and did not form a layer in the PL (Figure 5A–D and M,N). Furthermore, the orientation and radial morphology of Bergmann glia was disrupted at P7, a time point where granule cell migration is ongoing (Figure 5,C,D,G, and H). High power images demonstrated that the attachment of Bergmann glial end feet to the pial basement membrane was perturbed, with few glia maintaining their attachments in FGFR DKO (Figure 5G,H). Bergmann glia cell bodies were also located further away from the pial surface in FGFR DKO mice (Figure 5C,D). There was an apparent reduction in the density of radial glia/immature Bergmann glial in the cerebellum at E16.5, as demonstrated by Sox2 and by BLBP staining, but not as prominent as at P7 (Figure 5E,F,I,L). One guidance cue that plays an important role in cell migration and Purkinje cell layering in the cerebellum is the secreted protein Reelin (Goldowitz et al., 1997; Miyata et al., 1997). We found that Reelin was expressed, albeit at slightly reduced levels, in the cerebellum of FGFR DKO mice at E16.5, as compared to control littermates (Figure 5E,F,I,J).

2.5 Zic1/2 elucidates granule cell disruption during development

We hypothesize that disorganized and reduced Bergmann glia lead to the disruption of GC placement noticed in adult mutant tissue. In order to confirm a granule cell defect at P7, when Bergmann glia are disrupted and migration of granule cells is taking place, we immunostained for Zic1/2, a marker for granule cell precursors. In FGFR DKO mice, Zic1/2-positive cells were located between the external and inner granule cell layer, apparently halted in their migration; furthermore, no clear accumulation of Zic1/2 positive granule cell bodies in the incipient IGL was observed (Figure 6A–F).

In addition to the apparent differences in granule cell migration, Zic1/2 counts demonstrate a reduction in the pool of GCPs in mutant animals (Figure 6M). The reduction in GCPs accounts for the decreased cerebellar size. To further investigate whether there was a decrease in proliferation or survival due to absent FGFR1 and FGFR2 function, we labeled cells in S phase with BrdU using an acute injection protocol. We found that at P7 the layer of BrdU+ cells in the EGL appeared discontinuous and thinner in DKO mice compared to control mice (Figure 6G,H). The reduction in granule cells at P7 did not appear due to increased apoptosis since staining for activated Caspase 3 did not indicate an increase in apoptotic cells in the FGFR DKO mice (data not shown).

The reduction in proliferating and migrating granule cells could either be due to a failure of proliferation as they migrate, or also, due to a decrease in stem cell proliferation or maintenance at the upper rhombic lip. We performed a single BrdU injection at E14.5 and examined the number of BrdU+, Ki67+, and double-labeled cells in the rhombic lip 24 hours later at E15.5. We found no significant differences in BrdU+ (control = 0.082 cells/μm^2 ± 0.011 sem and FGFR DKO = 0.094 cells/μm^2 ± 0.023 sem, counts of matched images), Ki67+ (control = 0.053 cells/μm^2 ± 0.008 sem and FGFR DKO = 0.065 cells/μm^2 ± 0.018 sem), or double-labeled cells (control = 0.017 cells/μm^2 ± 0.003 sem and FGFR DKO =

0.029 cells/μm^2 ± 0.007 sem, Figure 6I,J). We also found no differences in Sox2 at E15.5 in the rhombic lip (Figure 6K,L).

2.6 Cerebellar abnormalities result in altered motor learning and gait in FGFR DKO mice

To test whether these cerebellar abnormalities may produce alterations in spatial and motor behavior, we assessed the performance of control and FGFR DKO mice on the rota-rod test. The rota-rod tests both the ability of mice to keep their posture on a rotating rod and their ability to improve motor performance over 3 testing days. The FGFR DKO mice had impaired performance on the rota-rod test when compared to littermate controls, showing less time on the rod in each trial and impaired ability to learn the motor behavior over three testing days (Figure 7A,B). Groups were compared using a general linear model with a test for repeated measures. A significant effect of genotype upon time spent on the rota-rod was observed between subjects ($p<0.001$, $F=28.96$, $df=1$). No significant effects were observed within subjects on rota-rod performance. Observation of the FGFR DKO mice also revealed that these mice appeared to have an abnormal gait. Analysis of paw-print patterns demonstrated a wider spacing of paw prints (4.58 ± 0.15 mm versus 4.12 ± 0.01 mm, $p=0.014$), as well as a disturbance in the forefoot and hindfoot step coordination (Figure 7C).

3. Discussion

The compound mutation of *Fgfr1* and *Fgfr2* driven by the *hGFAP-Cre* transgene causes abnormal cerebellar development. FGFR DKOs have decreased cerebellar volume and multiple cellular abnormalities that result in abnormal cerebellar lobule and layer formation. We found that FGFR DKO have a reduced number of Bergmann glia, and that those Bergmann glia that are present, have a lack of radial orientation with reduced attachment of glial end feet to the glia limitans at the cerebellar pia. FGFR DKO also have a reduction in GCPs, as assessed by Zic1/2 positive cells, and apparently arrested granule cell migration, with abnormal accumulation of misplaced granule cells in the ML. In addition, FGFR DKO show almost total absence of GABAergic cerebellar interneurons in the ML and of Purkinje neurons in the PL and their retention in the IGL, resulting in the lack of an organized Purkinje cell layer. This is also reflected by the failure of Pax2 positive interneurons to reach the developing ML in the same numbers as in the control mice. These multiple cytoarchitectural abnormalities result in a ML that is deficient in inhibitory GABA interneurons and instead contains granule cells and an IGL that is poorly demarcated from the ML and contains abnormal accumulation of inhibitory interneurons.

We hypothesize that the decrease in cerebellar volume is attributable to a dual defect, (1) a lower number of cerebellar Sox2+ precursors and immature Bergmann glia, and (2) a decrease in proliferation of GCPs in the EGL that give rise to granule cell neurons. We observed no decrease in Sox2+ and/or in BLBP+ cell number at E15.5, a modest decrease at E16.5 and a prominent decrease in the early postnatal (P7) cerebellum of FGFR DKO mice. Sox2 is a transcription factor expressed by both Bergmann glia and by GFAP+ astroglial cells that act as neuronal progenitors in the immature cerebellum. In the in the neonatal cerebellum, Sox2+ glia in the white matter produce Pax2+ GABAergic neuron precursors that migrate to the ML, where they eventually differentiate into stellate and basket interneurons (Silbereis et al., 2009), and those in the EGL produce a subset of granule cells (Silbereis et al., 2009). Hence, depletion of the Sox2+ cell population will likely affect the genesis of multiple neuronal cell types, consistent with the hypoplastic cerebellum. The generalized decrease in Sox2+ cells observed in FGFR DKOs in the absence of cell death suggests that FGFR signaling is required to maintain the proliferation or self-renewal of these precursors. FGFRs have already been shown to be important for the self-renewal of radial glia in the embryonic brain, cells that also express Sox2 and display antigenic

properties of astroglial cells, including BLBP expression (Kang et al., 2009; Ohkubo et al., 2004; Rash et al., 2011; Stevens et al., 2010a; Yoon et al., 2004).

We observed two distinct effects on granule cells in FGFR DKO. The first is a reduction in their proliferation, which is most significant at perinatal stages of development as these cells migrate into the cerebellar anlage. The second is the migratory effect, presumably caused by decreased number and disorganization of Bergmann glia (see below). The Bergmann glia phenotype of FGFR DKO mice is similar to, but more extensive than, the cerebellar phenotype of Notch RBP-J conditional mutants, which have truncated Bergmann glia fibers and reduced numbers of Bergmann glia arising after P14 (Komine et al., 2007). Interestingly, since the phenotype arises after granule cell migration is complete, Notch RBP-J mutants do not show malformation of cerebellar folia, in stark contrast to the FGFR DKO mice which have abnormal Bergmann glia as early as E16.5.

Granule cells arise from precursors in the rhombic lip. These precursors are targeted by the hGFAP-Cre transgene (Marino et al., 2000; Schuller et al., 2008). FGFR DKO mice have a no apparent reduction in proliferative cells in the rhombic lip at E15.5, but a reduction of proliferation in the EGL at P7. Furthermore, birthdating studies indicate that the number of BrdU and Ki67 double-labeled cells was not decreased at E15.5, suggesting that stem cell maintenance in the rhombic lip is unaffected, but rather, the amplification of GCPs in the EGL is decreased, as reflected in the decreased number of BrdU+ cells at P7. We hypothesize that this difference in granule cell precursor proliferation arises sometime after E15.5 and before P7.

Fgf8 activity at the isthmic organizer has been implicated in cerebellar vermis morphogenesis due to an early proliferative or patterning effect at the midline, possibly due to a widening of the roof plate (Basson et al., 2008; Xu et al., 2000). In contrast, in our mutant the most lateral sections and anterior lobules are most disrupted. Conditional deletion of the *engrailed2* gene at E10.5 and E14.5 also results in abnormal foliation of the cerebellum without altering lamination, which is independent from Fgf8 (Cheng et al.). However, the hGFAP-Cre transgene is active after E13.5, when the early cerebellar patterning is complete, and our studies indicate that morphogenetic defects are absent at E15.5 and most prominent after P7, suggesting that the abnormalities in cytoarchitecture detected in our mutant largely occur through later mechanisms. Thus, FGF ligands play different roles at multiple stages of cerebellar development.

The abnormal lamination of the cerebellum may arise as a secondary consequence of migratory defects in the main cerebellar cell types. The disrupted attachment of Bergmann glial fibers to the pial surface prevents glia from aligning and remaining by the surface. The decrease in immature Bergmann glial cell scaffold spanning the cerebellar cortex may secondarily produce abnormal granule cell placement in the ML by preventing granule cells in the EGL from migrating down the Bergmann glia fibers to the IGL, and possibly contribute to the misplacement of Purkinje neurons and dendrites. The importance of Bergmann glia to granule cell migration is demonstrated by the studies of astrotactin, a protein expressed by migrating GCPs. Antibodies directed against astrotactin, or mutation of the astrotactin gene, impede granule cell attachment to Bergmann glia and migration along their fibers (Adams et al., 2002; Hatten, 1999; Zheng et al., 1996). In FGFR DKO mutants, granule cells are arrested in pockets at the external portion of the cerebellar cortex.

An alternative explanation is that the migratory defects of GCP could be attributed to the disruption in Purkinje cells that is also observed in FGFR DKO mice. While the Purkinje neurons are not targeted by the hGFAP-Cre transgene, they fail to form a continuous PL in the mutant mice. Purkinje cells migrate from the IV ventricle to the cerebellar primordium

along radial glial fibers at E13–E17 (Yuasa et al., 1991), before granule cells. The failure to form the Purkinje cell plate is already evident at E16.5, when fewer calbindin positive Purkinje neurons are present in the cerebellar anlage of FGFR DKOs compared to control mice, suggesting that disrupted Bergmann glia fibers result in abnormally placed Purkinje cells. This migratory defect in turn would subsequently result in reduced EGL progenitor proliferation. Indeed, it has been suggested that molecular cues in the early EGL and cerebellar anlage, notably Reelin, direct the migration and positioning of Purkinje neurons (Goldowitz et al., 1997; Jensen et al., 2002; Miyata et al., 1997). GCPs express Reelin and Purkinje cells express Disabled-1, a signaling molecule that is normally downregulated by Reelin; thus, differentiating granule cells signal through the Reelin pathway to Purkinje cells (Miyata et al., 1997; Swanson et al., 2005). In FGFR DKOs, the displacement of many Purkinje cells in the IGL, and their failure to properly migrate and organize themselves into the PL, is similar to the phenotype of the *reeler* mouse. However, Reelin is only modestly reduced in FGFR DKO mice, and this decrease in Reelin expression may be simply a reflection of the decreased number of GCPs in FGFR DKO mice. Extracellular cues different than Reelin or other processes may contribute to the Purkinje cell phenotype in the cerebellum of FGFR DKO mice.

Hence, we hypothesize that is that the lack of FGFRs has a dual effect on cerebellar development: (1) decreases the number of Bergmann cells and other radial glia-like neurogenic precursors in the cerebellar parenchyma, leading to decreased cerebellar neurogenesis, and (2) through deficient glial cell attachment/morphology, causes altered neuronal migration. The misplacement of granule cells in the ML on the one hand, and of Purkinje and other inhibitory neurons in the IGL on the other, is likely to upset the circuitry between stellate and basket cells and the network of granule cell axons and Purkinje cell dendrites. The resultant disruption of Purkinje cell signaling, which is crucial to deliver messages to the deep cerebellar nuclei, could significantly alter cerebellar information processing and result in the mutant's abnormal performance on tests of motor coordination and motor learning.

4.0 Experimental Procedure

4.1 Transgenic mouse lines

All animal procedures in this study were performed in accordance with Yale Animal Resources Center and IACUC policies. Mice with conditional deletion of FGFR1 and FGFR2 were generated by mating mice carrying floxed alleles of *Fgfr1 and Fgfr2* genes ($Fgfr1^{f}$ and $Fgfr2^{f}$) to *hGFAP-Cre* transgenic mice (Zhuo et al., 2001) to generate $hGFAP\text{-}Cre;Fgfr1^{f/f};Fgfr2^{f/f}$ double mutants (Stevens et al., in press). Genotyping was performed on DNA obtained by tail biopsy. PCR was performed for the $Fgfr1^{f}$ allele, the $Fgfr2^{f}$ allele, and *hGFAP-Cre* allele. Recombination was assessed by the presence of the ROSA reporter allele by immunostaining or x-gal staining for immunofluorescence staining of β-galactosidase (β-gal) as previously described. Mice heterozygous for the *Gad67-GFP* knock-in allele ($Gad67^{+/GFP}$) were crossed to $Fgfr1^{f/f};Fgfr2^{f/f}$ mice to generate $Fgfr1^{f/f};Fgfr2^{f/f};Gad67^{+/GFP}$ mice. Female $Fgfr1^{f/f};Fgfr2^{f/f};Gad67^{+/GFP}$ mice were mated to $hGFAP\text{-}Cre;Fgfr1^{f/f};Fgfr2^{f/f};Gad67^{+/+}$ males resulting in 25% $hGFAP\text{-}Cre;Fgfr1^{f/f};Fgfr2^{f/f};Gad67^{+/GFP}$. The *Gad67-GFP* allele was genotyped by screening newborn pups for GFP under a fluorescent dissection microscope, or by PCR for the GFP allele.

4.2 Immunohistochemistry

Postnatal day 7 (P7), P14 and adult mice were perfused with 4% paraformaldehyde (PFA). Brains were dissected and fixed with 4% PFA overnight. Embryonic Day 15.5 (E15.5) or

16.5 (E16.5) mice were obtained from timed pregnancies. Embryos were dissected in cold Hanks balanced salt solution; brains were removed and fixed in 4%PFA with PBS overnight. Fixative was replaced with 20% sucrose for a 24-hour period. Postnatal brains were embedded/frozen in OCT until sectioned into 50 m free-floating sections. Embryonic brains were sectioned at 20 μm, directly onto slides. For BrdU assays, 100 mg/kg was administered one-hour prior to harvest for P7 animals, and 24 hours prior to harvest to the pregnant damn, for the E15.5 animals.

Sections were stained with the following primary antibodies: rabbit anti-activated caspase-3 (Cell Signaling, 9661), rabbit anti calretinin (SWANT), mouse anti parvalbumin (Sigma-Aldrich), mouse anti calbindin (Sigma-Aldrich), rabbit anti β-gal (Cappel), chicken anti-β-gal (abcam), rabbit anti GFP (Invitrogen), rabbit anti Pax2 (Zymed), Mash1 (ms anti-Mash1, M. Goetz), rabbit anti-Zic1/2 (Dr. Pazra), rabbit anti BLBP (Abcam), rat anti-BrdU (Accurate Chemicals), rabbit anti-Ki67 (Vector Labs), mouse anti-Reelin (Chemicon) rabbit anti-Sox2 (Chemicon), mouse anti-NeuN (Chemicon). Secondary antibodies were Alexa-conjugated (Invitrogen) or AMCA-conjugated (Vector) fluorescent labeled antibodies. Fluorescence images were examined using a Zeiss Apotome microscope and captured with a Hamamatsu ORCA camera.

4.3 Cresyl Violet

Sections were allowed to dry overnight, and followed by serial processing as follows: slides were rinsed with de-ionized water, soaked in cresyl violet stain for 20 minutes, passed through an increasing series of alcohol baths, and two xylene washes. Slides were coverslipped with Permount medium and imaged using a Zeiss Discovery V.8 stereo microscope with an Axiocam HR camera.

4.4 Cell Counts

Counts for BLBP, Sox2, and Zic1/2, were performed from images taken of matched sections of Lobule 1 (most lateral section containing lobule 1) of the cerebellum. The entire lobule was photographed at low magnification (20X) and area measurements were determined using axiovision software (Zeiss), positive cells in these images were marked using Photoshop. Data was analyzed by entering into Excel (Microsoft Office) and analyzed by student's t-test. Counts for BrdU/Ki67 and Sox2 were performed from images taken of matched sections of the rhombic lip and cerebellar anlage at 10X. Positive cells were marked using Photoshop, while areas were determined using axiovision software. Data was analyzed by entering into Excel (Microsoft Office) and analyzed by ANOVA using SPSS19.

4.5 Behavioral Testing

Motor learning was measured by the rota-rod task on three consecutive days, for six trials per day (AccuRotor, AccuScan Instruments, Columbus, OH). Six to eight mice (approximately 35 days old on the first day of testing) were tested per group. Mice were allowed to acclimate to the behavior testing room, prior to testing. Data was entered into excel files and exported to PAWS for analysis. Between subject and within subject analyses were performed using the General Linear Model for Repeated Measures. Paw print analysis was performed on 4 control and 4 FGFR DKO mice 2–5 month old mice. Paws were dipped in washable non-toxic paint and mice were placed on white paper. Gait width was determined by measuring the distance between left and right pawprints from three consecutive print pairs. Data was entered into excel and a student's t-test was performed.

Acknowledgments

We thank Eylem Ocal, Rebecca Deegan, and Jacob Kravitz for technical assistance. Zic1/2 antibody was generously shared by Dr. Pazra, Mash-1 was generously shared by Dr. Gotz. This work was supported by R01 MH067715 to FMV and K01 MH87845-2 to KMS.

References

Adams NC, Tomoda T, Cooper M, Dietz G, Hatten ME. Mice that lack astrotactin have slowed neuronal migration. Development. 2002; 129:965–72. [PubMed: 11861479]

Alcock J, Scotting P, Sottile V. Bergmann glia as putative stem cells of the mature cerebellum. Med Hypotheses. 2007; 69:341–5. [PubMed: 17337128]

Basson MA, Echevarria D, Ahn CP, Sudarov A, Joyner AL, Mason IJ, Martinez S, Martin GR. Specific regions within the embryonic midbrain and cerebellum require different levels of FGF signaling during development. Development. 2008; 135:889–98. [PubMed: 18216176]

Cheng Y, Sudarov A, Szulc KU, Sgaier SK, Stephen D, Turnbull DH, Joyner AL. The Engrailed homeobox genes determine the different foliation patterns in the vermis and hemispheres of the mammalian cerebellum. Development. 2010; 137:519–29. [PubMed: 20081196]

Fogarty MP, Emmenegger BA, Grasfeder LL, Oliver TG, Wechsler-Reya RJ. Fibroblast growth factor blocks Sonic hedgehog signaling in neuronal precursors and tumor cells. Proc Natl Acad Sci U S A. 2007; 104:2973–8. [PubMed: 17299056]

Gasser UE, Hatten ME. Central nervous system neurons migrate on astroglial fibers from heterotypic brain regions in vitro. Proc Natl Acad Sci U S A. 1990; 87:4543–7. [PubMed: 2352935]

Goldowitz D, Cushing RC, Laywell E, D'Arcangelo G, Sheldon M, Sweet HO, Davisson M, Steindler D, Curran T. Cerebellar disorganization characteristic of reeler in scrambler mutant mice despite presence of reelin. J Neurosci. 1997; 17:8767–77. [PubMed: 9348346]

Hatten ME. Central nervous system neuronal migration. Annu Rev Neurosci. 1999; 22:511–39. [PubMed: 10202547]

Jensen P, Zoghbi HY, Goldowitz D. Dissection of the cellular and molecular events that position cerebellar Purkinje cells: a study of the math1 null-mutant mouse. J Neurosci. 2002; 22:8110–6. [PubMed: 12223565]

Joyner AL, Liu A, Millet S. Otx2, Gbx2 and Fgf8 interact to position and maintain a mid-hindbrain organizer. Current Opinion in Cell Biology. 2000; 12:736–41. [PubMed: 11063941]

Kang W, Wong LC, Shi SH, Hebert JM. The Transition from Radial Glial to Intermediate Progenitor Cell Is Inhibited by FGF Signaling during Corticogenesis. J Neurosci. 2009; 29:14571–14580. [PubMed: 19923290]

Komine O, Nagaoka M, Watase K, Gutmann DH, Tanigaki K, Honjo T, Radtke F, Saito T, Chiba S, Tanaka K. The monolayer formation of Bergmann glial cells is regulated by Notch/RBP-J signaling. Dev Biol. 2007; 311:238–50. [PubMed: 17915208]

Li JY, Lao Z, Joyner AL. Changing requirements for Gbx2 in development of the cerebellum and maintenance of the mid/hindbrain organizer. Neuron. 2002; 36:31–43. [PubMed: 12367504]

Lin Y, Chen L, Lin C, Luo Y, Tsai RY, Wang F. Neuron-derived FGF9 is essential for scaffold formation of Bergmann radial fibers and migration of granule neurons in the cerebellum. Dev Biol. 2009; 329:44–54. [PubMed: 19232523]

Liu A, Losos K, Joyner AL. FGF8 can activate Gbx2 and transform regions of the rostral mouse brain into a hindbrain fate. Development. 1999; 126:4827–38. [PubMed: 10518499]

Liu A, Li JY, Bromleigh C, Lao Z, Niswander LA, Joyner AL. FGF17b and FGF18 have different midbrain regulatory properties from FGF8b or activated FGF receptors. Development. 2003; 130:6175–85. [PubMed: 14602678]

Lutolf S, Radtke F, Aguet M, Suter U, Taylor V. Notch1 is required for neuronal and glial differentiation in the cerebellum. Development. 2002; 129:373–85. [PubMed: 11807030]

Machold RP, Kittell DJ, Fishell GJ. Antagonism between Notch and bone morphogenetic protein receptor signaling regulates neurogenesis in the cerebellar rhombic lip. Neural Develop. 2007; 2:5.

Maricich SM, Herrup K. Pax-2 expression defines a subset of GABAergic interneurons and their precursors in the developing murine cerebellum. Journal of Neurobiology. 1999; 41:281–94. [PubMed: 10512984]

Marino S, Vooijs M, van Der Gulden H, Jonkers J, Berns A. Induction of medulloblastomas in p53-null mutant mice by somatic inactivation of Rb in the external granular layer cells of the cerebellum. Genes Dev. 2000; 14:994–1004. [PubMed: 10783170]

Martinez S, Crossley PH, Cobos I, Rubenstein JLR, Martin GR. FGF8 induces formation of an ectopic isthmic organizer and isthmocerebellar development via a repressive effect on Otx2 expression. Development. 1999; 126:1189–1200. [PubMed: 10021338]

Milosevic A, Goldman JE. Potential of progenitors from postnatal cerebellar neuroepithelium and white matter: lineage specified vs. multipotent fate. Mol Cell Neurosci. 2004; 26:342–53. [PubMed: 15207858]

Miyata T, Nakajima K, Mikoshiba K, Ogawa M. Regulation of Purkinje cell alignment by reelin as revealed with CR-50 antibody. J Neurosci. 1997; 17:3599–609. [PubMed: 9133383]

Ohkubo Y, Uchida AO, Shin D, Partanen J, Vaccarino FM. Fibroblast growth factor receptor 1 is required for the proliferation of hippocampal progenitor cells and for hippocampal growth in mouse. J Neurosci. 2004; 24:6057–69. [PubMed: 15240797]

Rash BG, Lim HD, Breunig JJ, Vaccarino FM. FGF signaling expands embryonic cortical surface area by regulating Notch-dependent neurogenesis. J Neurosci. 2011; 31:15604–17. [PubMed: 22031906]

Rios I, Alvarez-Rodriguez R, Marti E, Pons S. Bmp2 antagonizes sonic hedgehog-mediated proliferation of cerebellar granule neurones through Smad5 signalling. Development. 2004; 131:3159–68. [PubMed: 15197161]

Sato T, Nakamura H. The Fgf8 signal causes cerebellar differentiation by activating the Ras-ERK signaling pathway. Development. 2004; 131:4275–85. [PubMed: 15294862]

Schuller U, Heine VM, Mao J, Kho AT, Dillon AK, Han YG, Huillard E, Sun T, Ligon AH, Qian Y, Ma Q, Alvarez-Buylla A, McMahon AP, Rowitch DH, Ligon KL. Acquisition of granule neuron precursor identity is a critical determinant of progenitor cell competence to form Shh-induced medulloblastoma. Cancer Cell. 2008; 14:123–34. [PubMed: 18691547]

Schwaller B, Meyer M, Schiffmann S. 'New' functions for 'old' proteins: the role of the calcium-binding proteins calbindin D-28k, calretinin and parvalbumin, in cerebellar physiology. Studies with knockout mice. Cerebellum. 2002; 1:241–58. [PubMed: 12879963]

Silbereis J, Cheng E, Ganat YM, Ment LR, Vaccarino FM. Precursors with glial fibrillary acidic protein promoter activity transiently generate GABA interneurons in the postnatal cerebellum. Stem Cells. 2009; 27:1152–63. [PubMed: 19418461]

Smith KM, Ohkubo Y, Maragnoli ME, Rasin MR, Schwartz ML, Sestan N, Vaccarino FM. Midline radial glia translocation and corpus callosum formation require FGF signaling. Nat Neurosci. 2006; 9:787–97. [PubMed: 16715082]

Solecki DJ, Liu XL, Tomoda T, Fang Y, Hatten ME. Activated Notch2 signaling inhibits differentiation of cerebellar granule neuron precursors by maintaining proliferation. Neuron. 2001; 31:557–68. [PubMed: 11545715]

Spassky N, Han YG, Aguilar A, Strehl L, Besse L, Laclef C, Ros MR, Garcia-Verdugo JM, Alvarez-Buylla A. Primary cilia are required for cerebellar development and Shh-dependent expansion of progenitor pool. Dev Biol. 2008; 317:246–59. [PubMed: 18353302]

Stevens HE, Smith KM, Maragnoli ME, Fagel D, Borok E, Shanabrough M, Horvath TL, Vaccarino FM. Fgfr2 is required for the development of the medial prefrontal cortex and its connections with limbic circuits. J Neurosci. 2010a; 30:5590–602. [PubMed: 20410112]

Stevens HE, Smith KM, Rash BG, Vaccarino FM. Neural stem cell regulation, fibroblast growth factors, and the developmental origins of neuropsychiatric disorders. Front Neurosci. 2010b:4.

Swanson DJ, Tong Y, Goldowitz D. Disruption of cerebellar granule cell development in the Pax6 mutant, Sey mouse. Brain Res Dev Brain Res. 2005; 160:176–93.

Tamamaki N, Yanagawa Y, Tomioka R, Miyazaki J, Obata K, Kaneko T. Green fluorescent protein expression and colocalization with calretinin, parvalbumin, and somatostatin in the GAD67-GFP knock-in mouse. J Comp Neurol. 2003; 467:60–79. [PubMed: 14574680]

Trokovic R, Trokovic N, Hernesniemi S, Pirvola U, Vogt Weisenhorn DM, Rossant J, McMahon AP, Wurst W, Partanen J. FGFR1 is independently required in both developing mid- and hindbrain for sustained response to isthmic signals. Embo J. 2003; 22:1811–23. [PubMed: 12682014]

Wechsler-Reya RJ, Scott MP. Control of neuronal precursor proliferation in the cerebellum by Sonic Hedgehog. Neuron. 1999; 22:103–14. [PubMed: 10027293]

Xu J, Liu Z, Ornitz DM. Temporal and spatial gradients of Fgf8 and Fgf17 regulate proliferation and differentiation of midline cerebellar structures. Development. 2000; 127:1833–43. [PubMed: 10751172]

Yoon K, Nery S, Rutlin ML, Radtke F, Fishell G, Gaiano N. Fibroblast growth factor receptor signaling promotes radial glial identity and interacts with Notch1 signaling in telencephalic progenitors. J Neurosci. 2004; 24:9497–506. [PubMed: 15509736]

Yuasa S, Kawamura K, Ono K, Yamakuni T, Takahashi Y. Development and migration of Purkinje cells in the mouse cerebellar primordium. Anat Embryol (Berl). 1991; 184:195–212. [PubMed: 1724357]

Zervas M, Millet S, Ahn S, Joyner AL. Cell behaviors and genetic lineages of the mesencephalon and rhombomere 1. Neuron. 2004; 43:345–57. [PubMed: 15294143]

Zheng C, Heintz N, Hatten ME. CNS gene encoding astrotactin, which supports neuronal migration along glial fibers. Science. 1996; 272:417–9. [PubMed: 8602532]

Zhuo L, Theis M, Alvarez-Maya I, Brenner M, Willecke K, Messing A. hGFAP-cre transgenic mice for manipulation of glial and neuronal function in vivo. Genesis. 2001; 31:85–94. [PubMed: 11668683]

Highlights

- Fgfr1 and Fgfr2 double knockout mice (FGFR DKO) have greatly reduced cerebellar size and decreased granule cell numbers.
- FGFR DKO have reduced proliferation of glial precursors and granule cell precursors
- In FGFR DKO mice, the inward migration of granule cells and outward migration of Purkinje neurons and GABA interneurons were arrested, likely due to altered number and morphology of Bergmann glia
- The disrupted cerebellar size and laminar architecture impairs motor learning and coordination in FGFR DKO mice.

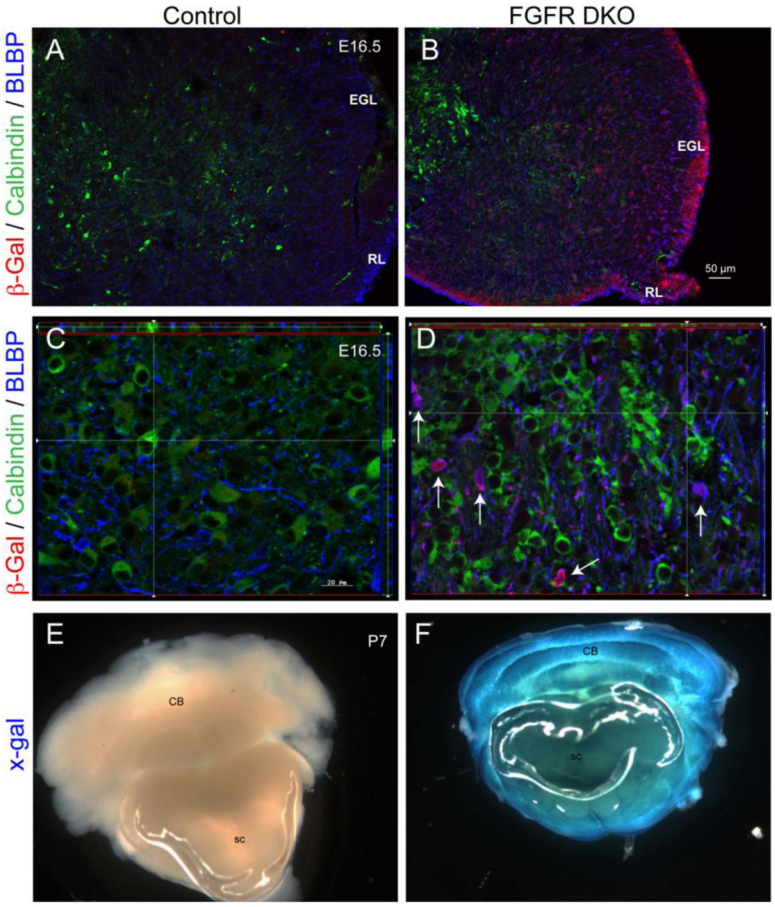

Figure 1. Characterization of *hGFAP-Cre* mediated recombination of the *ROSA26R* reporter locus in FGFR DKO mice by β-galactosidase (β-gal) detection

Immunostaining for β-gal (green) in the cerebellar anlage of E16.5 Cre-negative control (**A**) and FGFR DKO (**B**) littermates. Triple immunostaining for β-gal reporter (red), calbindin (green), and Blbp (blue) in control (A,**C**) and FGFR DKO mutant (B,**D**) littermates. Robust β-gal reporter staining is observed in the external granular layer (EGL) and rhombic lip (RL). High magnification images (D) indicate that calbindin positive cells lack β-gal expression, whereas Blbp positive cells are positive for β-gal (arrows). Detection of β-gal activity in P7 cerebellum by X-gal staining shows lack of activity in Cre-negative control animals (**E**), and extensive X-gal staining throughout the Cerebellum (CB) and Spinal Cord (SC) of FGFR DKO mice (**F**).

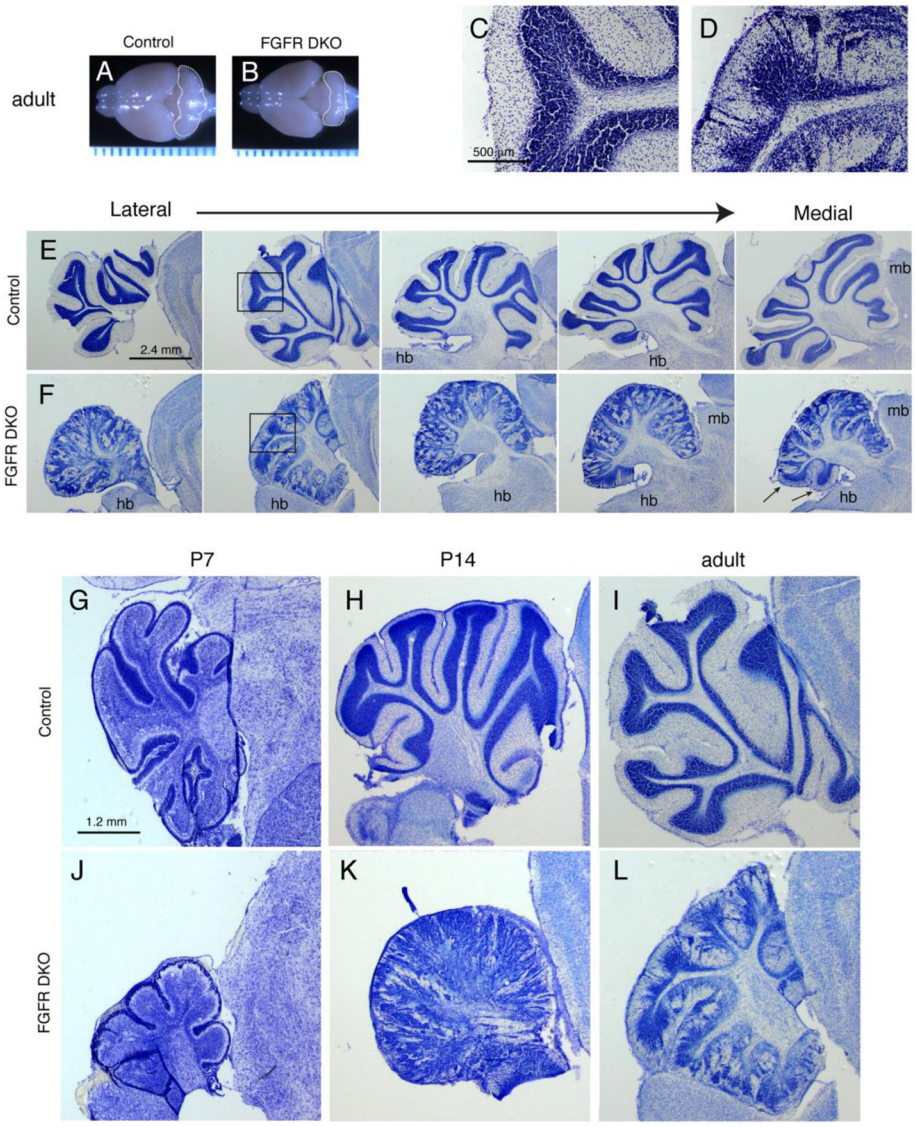

Figure 2. Fgfr1 and Fgfr2 Double mutants show decreased cerebellar volume and abnormal cerebellar lobule and layer morphology

Whole mount view of adult (3 month old) brains of control (**A**) and FGF DKO (**B**) mice demonstrate the decreased size of the FGFR DKO cerebellum (outlined). Ruler units are in mm. Cresyl violet staining of sagittal sections from adult control (**C,E**) and FGFR DKO (**D,F**) mice demonstrate the abnormal laminar formation (compare **C** and **D**), and the malformed cerebellar cortex of FGFR DKO adults in the lateral to medial extent (**E**,**F**). The disruption occurs in a gradient with the most lateral sections and anterior lobules most disrupted. Arrows indicate posterior lobules on a medial section, which are spared from significant disruption. Developmental analysis of postnatal cerebellar morphology from P7 (**G** and **J**), P14 (**H** and **K**), and adult (**I** and **L**) control (**G**–**I**) and FGFR DKO (**J**–**L**) mice. Hindbrain, hb; midbrain, mb; ml, molecular layer; igl, internal granular layer.

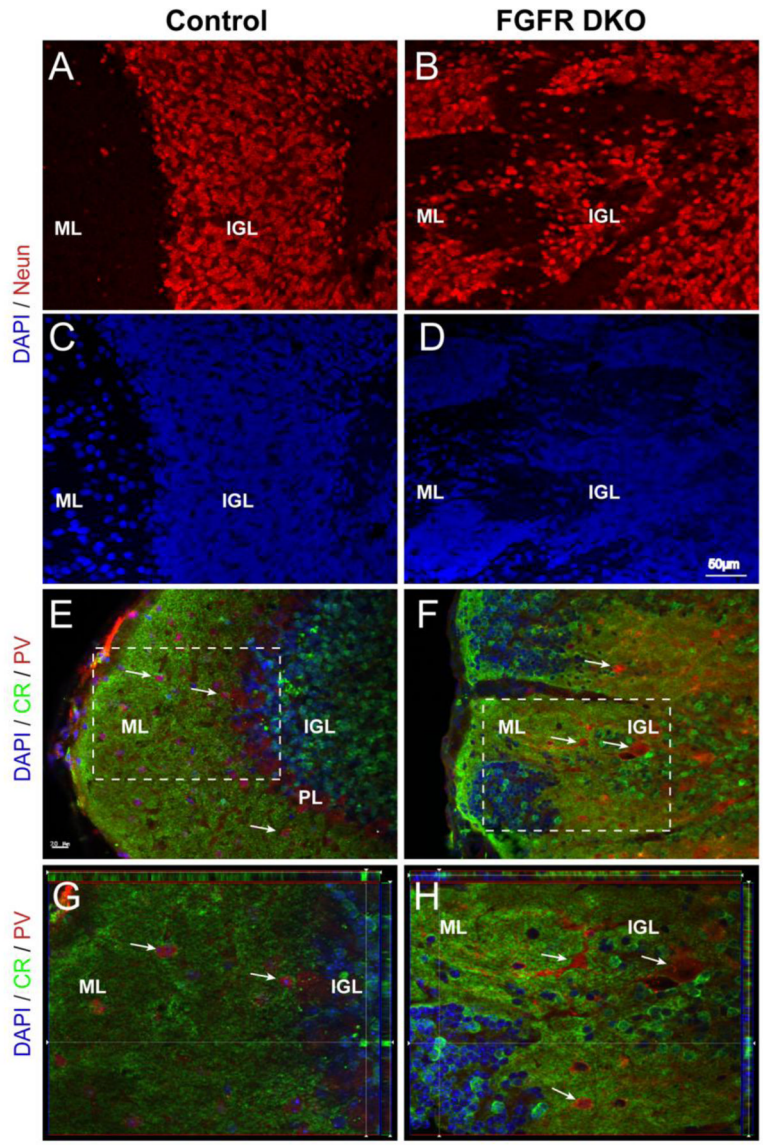

Figure 3. Clusters of misplaced cells in the cerebellar cortex of adult FGFR DKO mice are granule cell neurons

Sagittal sections of adult control (**A** and **C**) and FGFR DKO (**B** and **D**) were immunostained for the neuronal marker NeuN (**A** and **B**), while all nuclei were stained with DAPI (**C**, **D**). The location of NeuN positive cells in the control demonstrates a clear transition from the cell dense IGL to the ML. In the mutant, labeled NeuN cells are scattered throughout the lobule with no clear demarcation between the IGL and ML. (**EH**) Granule cells were identified by Calretinin (CR) immunostaining and Purkinje neurons and interneurons were identified with Parvalbumin (PV) in control (**E** and **G)** and FGFR DKO mice (**F** and **H**). In the control, CR cell body staining is limited to the IGL and excluded from the ML (**E**, inset shown in G) whereas in the mutant cerebellum, there are Calretinin-positive cells throughout the lobule (**F**, inset shown in **H**) and in isolated pockets in the ML. The absence of a clear boundary between the IGL and ML is indicated by pockets of Calretinin+ cells located at the most external portion of the lobule. PV staining was present in the PL and in ML in control

animals (**E**,**G**), in comparison to FGFR DKO mice, in which most PV+ cells were dispersed in the IGL away from the ML, with few PV cells in the molecular layer (**F**,**H**).

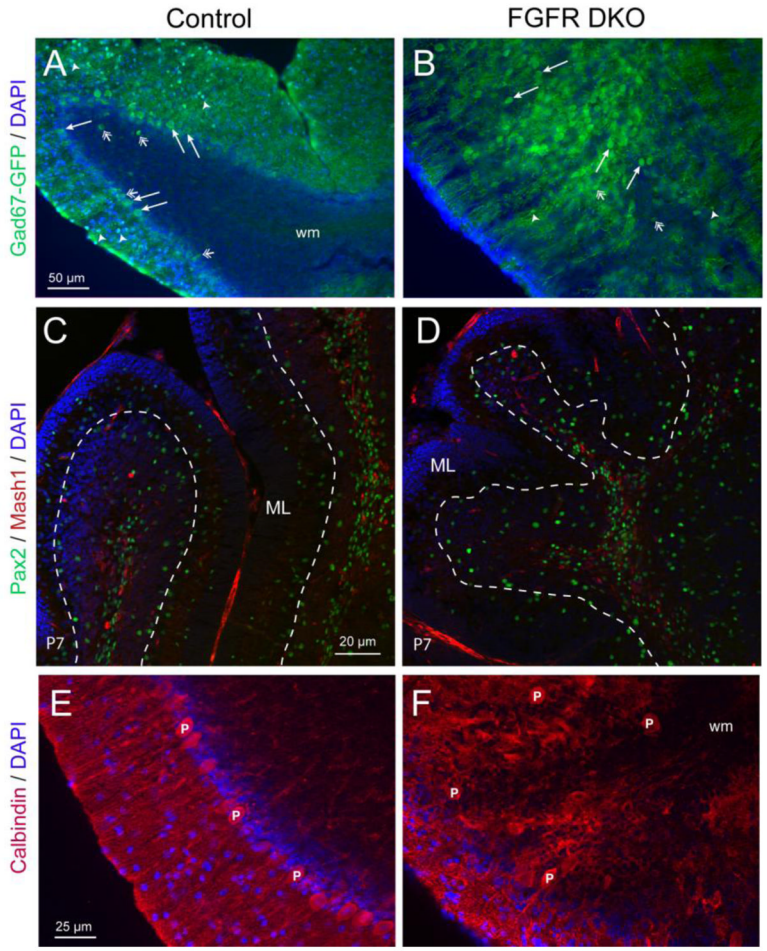

Figure 4. Purkinje neurons are misplaced and ML interneurons are decreased in FGFR DKO mice

Cerebellar interneurons of adult Control (**A**) and FGFR DKO (**B**) were imaged by immunofluorescence for GFP in 3 month old mice with the GAD67-GFP transgene. GFP labels both the interneurons of the ML (white arrowheads), Purkinje neurons (arrows) and Golgi cells (open arrows). In the control (**A**), large cell body Purkinje cells are present in the PL, while in the FGFR DKO (**B**), large cell body interneurons are prevalent internally and small body interneurons are nearly absent from the ML. Pax2 (green) and Mash1 (red) were used to visualize migrating interneurons in P7 control (**C**) and FGFR DKO mice (**D**). White-dashed line marks the separation between the PL/GCL and ML. Purkinje neurons were also visualized by calbindin immunostaining (red) in control (**E**) and FGFR DKO (**F**) mice. DAPI (blue) was used to visualize all nuclei. Calbindin-labeled interneurons in the control align in the Purkinje layer and extend red-labeled dendrites into the molecular layer (**C**). In the mutant (**F)** calbindin-positive interneurons are not uniformly aligned and have no clear, unidirectional pattern of dendrite extension.

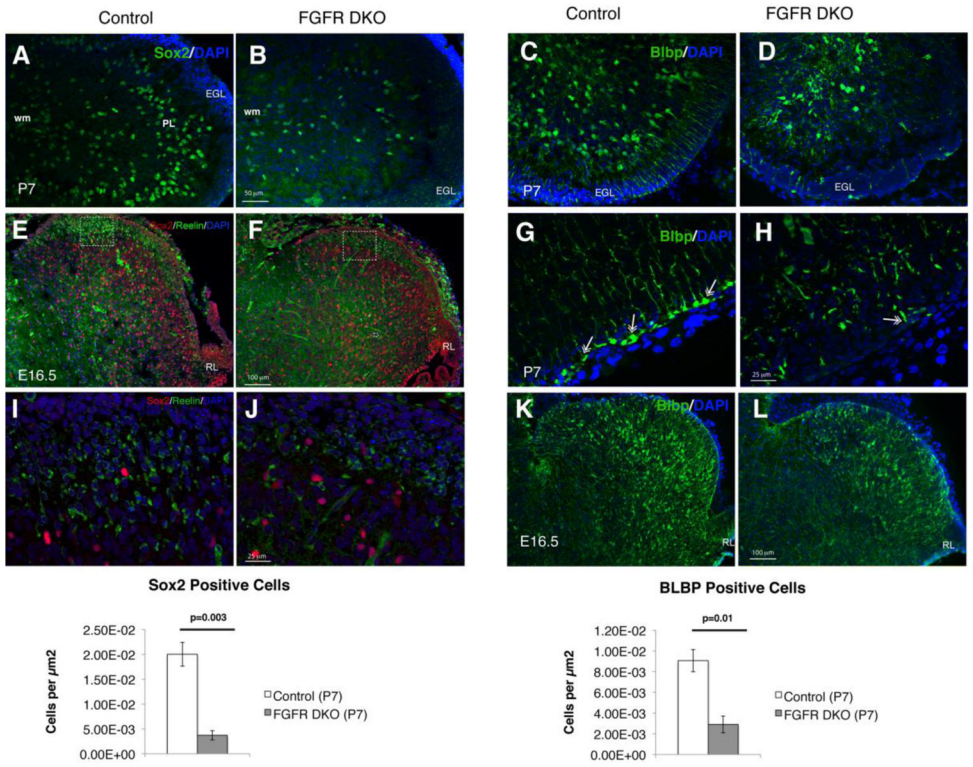

Figure 5. The severely disrupted cerebellum in adult FGFR DKO mice is a result of decreased number and altered radial orientation of glial cells

Immunofluorescence staining for Sox2 at P7 in Control (**A**) and FGFR DKO mice (**B**). FGFR DKO had significantly fewer Sox2+ cells than control littermates (**M**). Immunofluorescence staining for BLBP in control (**C**,**G**) and FGFR DKO mice (**D**,**H**) at P7 demonstrates that in FGFR DKO animals (**H**) the Bergmann glia are significantly reduced in number (**N**), their cell bodies are further inside from the EGL than in the control, and there is a relative lack of radial glial fibers traversing the EGL and forming glial end feet attachments (double headed arrows in **G** and **H**) compared to controls. Sox2 and Reelin immunostaining of control (**E**,**I**) and FGFR DKO (**F**,**J**) embryos at E16.5 demonstrate a mild decrease in both Sox2 positive and Reelin positive cell bodies. Squares in **E** and **F** indicate location of high power images in **I** and **J**. BLBP staining in E16.5 embryos of control (**K**) and FGFR DKO (**L**) mice demonstrate that the defects in Bergmann glia number and morphology arise embryonically.

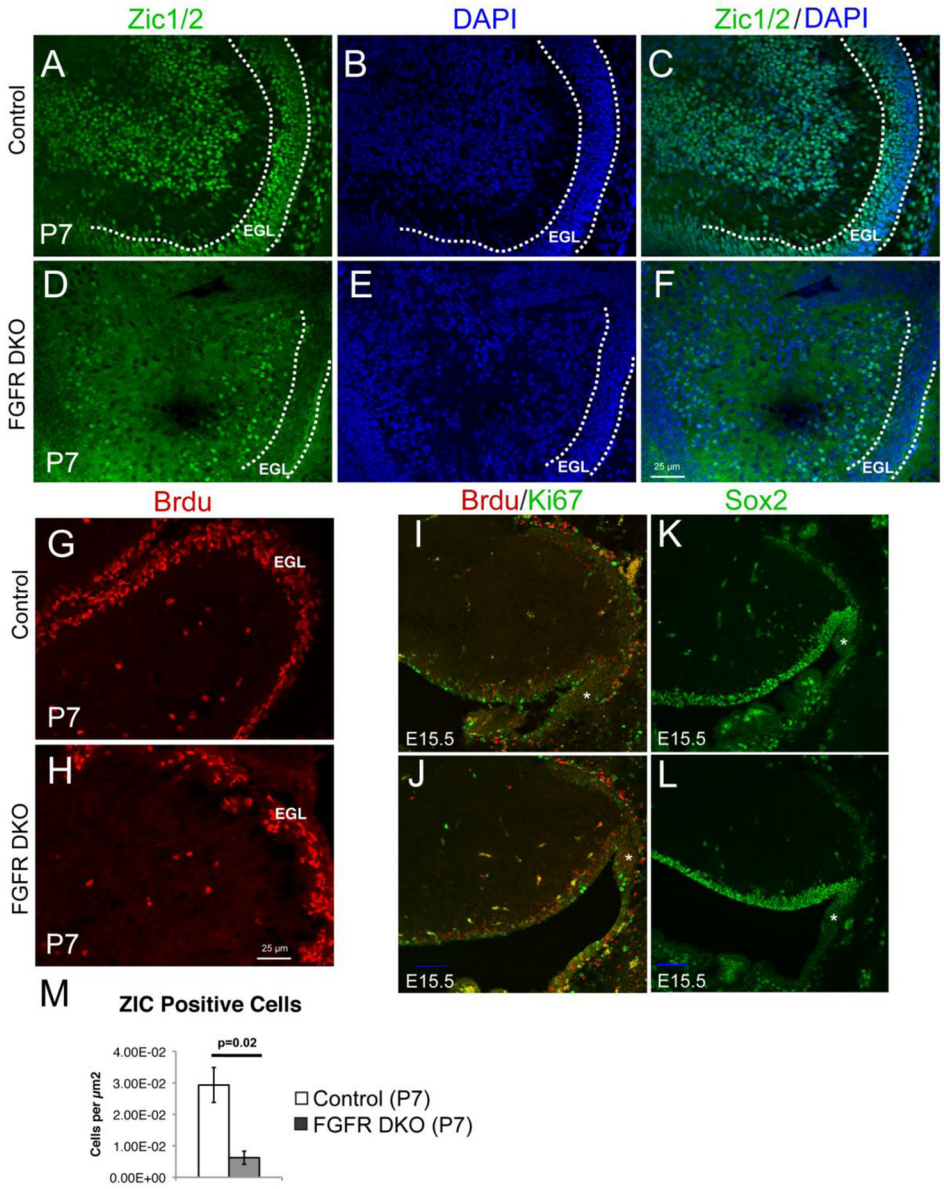

Figure 6. Cerebellar Granule cell number is decreased and migration is disrupted in FGFR DKO mice

Immunofluorescence for Zic1/2 in P7 mice was used to visualize migrating granule cell neurons. Control mice (**A**–**C**) had significantly more Zic1/2 positive granule cells than FGFR DKO mice (**D**–**F**, **M**). DAPI staining showing abnormal layer distribution of the Zic1/2 positive cells in FGFR DKO (**E**, **F**) as compared to controls (**B**, **C**). EGL is outlined by a dashed line. Compared to control mice (**G**), the number of actively dividing BrdU-labeled cells appears reduced in EGL of the FGFR DKO mice (**H**) at P7, indicating a decrease in proliferation in GCPs. At E15.5, 24 hours after BrdU administration, similar numbers or BrdU+, Ki67+, and double-labeled cells were observed in the rhombic lip (asterisk) of control (**I**) and FGFR DKO embryos (**J**). No differences in Sox2 positive cells were observed in the rhombic lip of E15.5 control (**K**) and FGFR DKO embryos (**L**). Scale bar in J and L is 20μm.

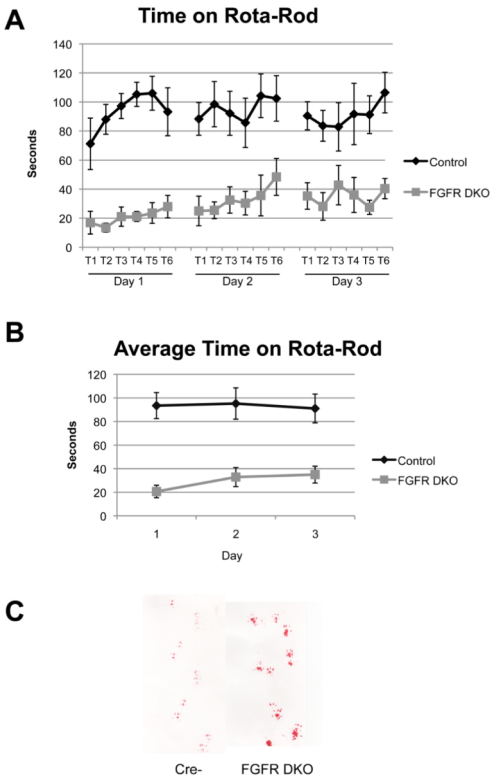

Figure 7. Cerebellar layer and size disruptions lead to decreased ability to perform motor and motor learning tasks

The rota-rod tests both the ability of mice to keep their posture on a rotating rod and their ability to improve motor performance over 3 testing days. The FGFR DKO mice had impaired performance on the rota-rod test when compared to littermate controls, showing less time on the rod in each trial, and did not learn the motor behavior over three testing days (**A**,**B**). Paw print test demonstrating abnormal gait of FGFR DKO mice in comparison to controls (**C**).